

Symbiotic Novae

Ulisse Munari¹ 

*INAF National Institute of Astrophysics, Astronomical Observatory of
Padova, 36012 Asiago (VI), Italy, (E-mail: ulisse.munari@inaf.it)*

Received: May 1, 2020; Accepted: July 28, 2020

Abstract. (Invited Review) According to modern definition, a symbiotic nova is an otherwise normal nova (i.e. powered by *explosive* thermonuclear burning) that erupts within a symbiotic star, which is a binary where a WD accretes from a cool giant companion. Guided primarily by the very well observed eruptions of RS Oph in 2006 and 2021, and that of V407 Cyg in 2010, we describe the main multi-wavelength properties of symbiotic novae and their relation to classical novae, and propose a 3D model structure that identifies the emitting source location for hard and supersoft X-rays, radio synchrotron and thermal, permitted and forbidden emission lines. Very few symbiotic novae are known in the Galaxy, and we compile a revised catalog based on firm astrometric identification. The exciting prospect of an imminent new outburst of T CrB is also discussed.

Key words: binaries: symbiotic – novae, cataclysmic variables – circumstellar matter – jets and outflows – catalogs

1. A modern definition for symbiotic novae

Traditionally (eg. Gaposchkin, 1957; Allen, 1980; Kenyon, 1986; Warner, 1995), the term 'symbiotic nova' has indicated a symbiotic star undergoing a large amplitude ($\Delta V \geq 4$ mag) and very long lasting outburst (several decades to a century), clearly distinct from the smaller amplitude ($\Delta V \sim 2$ mag) and much faster eruptions (from several months to a few years) characterizing most of the symbiotic binaries and usually referred to as 'ZAND' events, from the prototype Z And that has gone through several of them in its recorded history (eg. Tomov et al., 2016; Skopal et al., 2020). Over the last 10-20 yrs the accepted meaning has however drastically changed to

a symbiotic nova is an otherwise normal nova [i.e. powered by explosive thermonuclear burning] that erupts within a symbiotic binary

which we will adopt in this review. Classical novae and symbiotic novae share similar properties in the way their white dwarfs (WD) accrete mass and then ignite the explosive burning. A classical nova is a compact interacting binary, where a WD accretes (usually via Roche lobe overflow and formation of an accretion disk) from a low-mass red dwarf companion (RD), orbiting in a few

hours at a distance of about a Solar radius. In the case of a symbiotic binary the companion to the WD is a red giant (RG), and to accommodate its much larger dimensions the orbital separation widens to a few astronomical units and the orbital period increases to a few years.

For both the classical and symbiotic novae, the accreted material goes accumulating in electron-degenerate conditions on the surface of the WD; diffusion from the outer layers of the WD allows enrichment in CNO nuclei (ensuing stronger explosions). Once the pressure at the base of the accumulated shell reaches a critical value around 10^{20} dyn/cm², nuclear burning of the accreted material sets in. Given its electron-degenerate state ($P \propto \rho^\beta$), the shell does not initially react by expanding to the increase in temperature, with the consequent ramping in energy released by the nuclear reactions ($\epsilon_{\text{CNO}} \propto T^{17}$) which leads to further increase in temperature. Within a few minutes, the temperature reaches the Fermi value (of the order of 10^8 K), at which point the electron degeneracy is suddenly lifted ($P \propto \rho T$), and the hyper-hot material in the shell violently expands at velocities in excess of the escape velocity from the WD ($v_e = \sqrt{2GM/R} \sim 9100$ km sec⁻¹ at $M=1.25 M_\odot$; [Arseneau et al. \(2024\)](#)), effectively terminating the TNR (eg. [Starrfield, 1989](#); [Starrfield et al., 2008](#)). Not the entire shell is however expelled, and the nuclear burning can continue (now in thermal equilibrium) in what has been left of the shell on the surface of the WD, a phase lasting for weeks–months and characterized by supersoft X-rays emission, which become observable when the ejecta turn optically-thin (eg. [Schwarz et al., 2011](#)).

The paths followed by classical and symbiotic novae diverge at this point, at the time when the shell is violently expelled by the WD. Unbind from the system, the ejected material travels the WD–RD orbital separation of a classical nova in a matter of minutes, after which (and for the time being) it basically keeps expanding on free ballistic trajectories into the circumstellar void, as beautifully demonstrated by Nova Per 1901 ([Liimets et al., 2012](#)) and other novae with spatially resolved ejecta ([O’Brien & Bode, 2008](#)). In a symbiotic nova instead, the circumstellar space up to hundreds of AU is filled by the thick and slow wind of the RG, and the fast expanding ejecta have to plow their way through it ([Sokoloski et al., 2008](#); [Evans et al., 2008](#)). This results in a violent and efficient deceleration of the ejecta, and the associated massive shock-fronts power emission from the highest energies probed by Cherenkov telescopes all the way down to the synchrotron emission dominating at radio wavelengths. The first nova ever detected in γ -rays (by the *Fermi*-LAT satellite) has been, not incidentally, the symbiotic nova V407 Cyg in 2010 ([Abdo et al., 2010](#)).

The literature about observations and modeling of nova explosions is very rich, and well beyond the possibility of a balanced citation in a short review like the present one. Excellent summaries may be found in the books and proceedings of conferences devoted specifically to novae, like those edited by [Bode & Evans \(1989\)](#), [Cassatella & Viotti \(1990\)](#), [Hernanz & José \(2002\)](#), [Bode & Evans \(2008\)](#), [Saikia & Anupama \(2012\)](#), and [Woudt & Ribeiro \(2014\)](#).

OLD MEANING FOR 'SYMBIOTIC NOVAE'. Before moving on, some words are in order about the *traditional* meaning of the term 'symbiotic nova', which is still - although rarely - in use. In the life-cycle of a typical symbiotic star as proposed by [Munari \(2019\)](#), the longest intervals are spent accreting onto the WD (at highly variable rates). In the (great) majority of the symbiotic stars the accreted envelope is non-degenerate, primarily because of the low mass of the WD. Once the conditions for nuclear burning are reached, the burning ignites non-explosively and continues in thermal equilibrium as long as enough hydrogen fuel is present in the shell, a phase lasting decades to centuries ([Iben, 1982](#); [Fujimoto, 1982b,a](#); [Kenyon & Truran, 1983](#)). The rise to optical maximum takes a few years to complete (~ 3 yrs for V1016 Cyg and V3268 Sgr): these are the symbiotic novae according to the old definition (for which we propose the name SETE standing for Symbiotic stars Erupting in Thermal-Equilibrium). The shell is *not* ejected and remains in hydrostatic equilibrium, progressively contracting in radius and slowly rising in surface temperature as the hydrogen fuel is consumed. Once the burning shell shrinks to the radius and temperature of the nuclei of planetary nebulae, accretion-induced ingestion by the shell of limited amounts of mass triggers short-lived ZAND outbursts (as observed in 2015 for AG Peg; [Tomov et al., 2016](#)). The exhaustion of the hydrogen fuel in the shell eventually stops the burning, the strong emission lines and ultraviolet continuum die away, and the symbiotic star (now broadly resembling a field single RG) resumes the long-lasting and quiet accretion phase in preparation for a new cycle.

2. A revised catalog of Symbiotic Novae

From the previous section, the main difference between classical and symbiotic novae resides in the nature of the companion to the WD: a red dwarf versus a red giant. Considering that in the infrared K band (*i*) cool dwarfs and cool giants differ by ~ 10 in absolute $M(K)$ magnitude, and (*ii*) the interstellar reddening plays a marginal role ($A(K)=0.43 \times E_{B-V}$ for M spectral types), and (*iii*) the sensitivity of the 2MASS JHK survey is high enough to detect a red giant anywhere in the Galaxy, it seems a good choice to investigate the distribution of novae in 2MASS K band to segregate symbiotic novae from classical ones.

We started by assembling various compilations of Galactic Novae (from IAU, SIMBAD, Bill Gray, Koji Mukai, and others) and proceeded with pruning them from mis-entries. For ex., FU Ori - the prototype of erupting pre-main sequence stars - is still listed as Nova Ori 1939. We therefore retained only the objects for which there is observational evidence of an *explosive* TNR event on a WD (which excludes SETE objects). Next, we tried to obtain accurate astrometric coordinates and a measure of their error by going to the original sources of the epoch (for ex., SIMBAD coordinates for Nova Sgr 1935 are those of an unrelated Mira variable, ~ 1 arcmin away from the true nova position, as clear from a find-

ing chart of the epoch). For novae up to 1985, the prime source for astrometric coordinates and finding charts is the reference catalogue and atlas of [Duerbeck \(1987\)](#), where in most cases the original discovery photographic plates were directly inspected and astrometrically measured in a modern way. For later novae, we went through the original discovery announcements (on IAUC, CBET, ATel, etc.), follow-up papers, and the catalog and atlas of CVs by [Downes & Shara \(1993\)](#) and [Downes et al. \(1997, 2001\)](#). The quoted coordinates were critically re-evaluated and their errors estimated in parallel with direct inspection of POSS scans and 2MASS maps. Only novae identified with a high degree of confidence and not in blend with field stars were retained. The surviving objects were then cross-matched with Gaia DR3 ([Gaia Collaboration, 2016, 2023](#)) looking for possible nearby, faint field stars that could interfere with a firm identification of the progenitor. After this further pruning, the Gaia DR3 coordinates were adopted and the final list of novae was cross-matched with the 2MASS catalog ([Skrutskie et al., 2006](#)) within 1arcsec radius (including correction for proper motion).

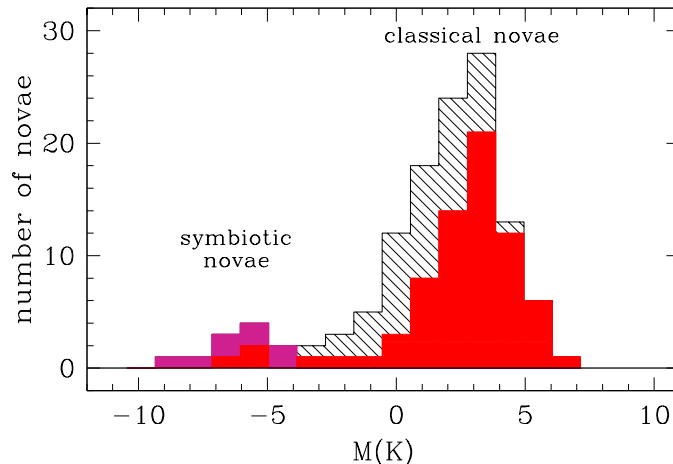


Figure 1. Distribution in absolute $M(K)$ magnitude of all validated thermonuclear runaway novae with an accurate astrometric identification. Those containing a red giant ($M(K) \leq -4$ mag) are listed in Tab. 1.

As a final step, the Gaia DR3 parallax was adopted to compute the absolute magnitude of novae in the K band ($2.2 \mu\text{m}$), which resulted in the distribution of Fig. 1. In this figure, the novae with an error on the parallax inferior to 25%, are plotted in red, those with a larger error are dashed. Various novae with a red giant are listed in Gaia DR3 with a too large uncertain in the parallax, and consequently we derived their distances as an average of independent estimates found in literature; these systems are plotted in purple in Fig. 1. No correction

Table 1. The symbiotic novae (novae with a red giant), corresponding to the objects with $M(K) \leq -4$ in Fig. 1.

Name	Outbursts	Gaia DR3						Galactic		2MASS	
		RA	DEC	π	$\sigma(\pi)$	BP	RP	long	lat	K_s	(J- K_s)
RS Oph	1898, 1933, 1958, 1967 1985, 2006, 2021	17 50 13.159	-06 42 28.48	0.373	0.023	11.44	9.38	19.80	10.37	6.50	1.134
V745 Sco	1897, 1937, 1989, 2014	17 55 22.226	-33 14 58.55	0.100	0.076	16.54	13.25	357.36	-4.00	8.26	1.78
V3890 Sgr	1962, 1990, 2019	18 30 43.288	-24 01 08.9	0.048	0.045	15.82	12.75	9.20	-6.44	8.26	1.57
T CrB	1866, 1946	15 59 30.162	+25 55 12.61	1.092	0.028	9.91	7.62	42.37	48.16	4.81	1.19
V407 Cyg	1936?, 2010	21 02 09.819	+45 46 32.73	0.247	0.117	16.14	10.19	86.98	-0.48	3.3	2.4
EU Sct	1949	18 56 13.127	-04 12 32.41	0.072	0.037	17.60	14.53	29.73	-2.98	10.80	1.45
V1172 Sgr	1951	17 50 23.657	-20 40 29.82	0.104	0.047	18.13	14.97	7.64	3.34	11.03	1.54
V5581 Sgr	2009	17 44 08.460	-26 05 48.00	-0.04	0.145	20.34	13.96	2.25	1.76	7.92	2.09
V5590 Sgr	2012	18 11 03.700	-27 17 29.43	0.129	0.032	12.92	11.22	4.23	-4.04	7.35	1.95
V1534 Sco	2014	17 15 46.881	-31 28 30.31	0.113	0.070	17.91	14.10	354.33	3.99	9.58	1.68
V1708 Sco	2020	17 23 41.935	-31 03 07.60	0.073	0.071	18.66	14.72	355.65	2.84	9.75	1.88

for reddening is applied because it is reliably *measured* (not simply guessed) only for a tiny minority of all novae, and its impact - which is at the level of a few tenths of a magnitude at most - does not affect at all the distinction between classical and symbiotic novae in Fig. 1.

The distribution in Fig. 1 is clearly bi-modal. The more numerous group, which is that of classical novae (those with a red dwarf), presents a Gaussian-like distribution centered at $M(K)=+3.2$ mag. It is worth noticing that this value is about 1 mag brighter than the absolute K magnitude of main sequence K-type stars, suggesting that the same accretion disk that dominates the UV and optical energy distribution of old novae (Cassatella et al., 1990, 2004) extends its influence also into the infrared.

The smaller group in Fig. 1, is that of symbiotic novae, with a mean absolute magnitude of $M(K) \approx -5.8$ mag, which is close to the mean $M(K) = -5.9$ mag derived by Munari et al. (2021) for the accreting-only symbiotic stars. This similarity can be read as an indication that the population of red giants in field symbiotic stars and in symbiotic novae is the same, and presumably also their mass loss rates. The symbiotic novae in Fig. 1 (those with $M(K) \leq -4.0$ mag) are listed in Tab. 1, with quoted values taken from Gaia DR3 and 2MASS catalogues. Those with more than one recorded eruption (*symbiotic recurrent* novae) are listed at the top.

3. The distinctive presence of the red giant wind

We remarked above how the primary differences between classical and symbiotic novae originate from the wind of the red giant filling the circumstellar space of

symbiotic novae, and how it interacts with the radiation output and the fast ejecta of the outbursting WD.

3.1. Flash ionization of the red giant wind

A feature unique to symbiotic novae actually manifests even before the fast ejecta begins slamming onto the pre-existing slow wind of the RG. It originates from the strong UV-flash originating from the burning shell during the TNR and its immediate aftermath. The flash is really short-lived: in the nova models by Starrfield et al. (2008), the shell surface temperature drops to 1×10^5 K in ~ 300 sec and ~ 500 sec for WDs of 1.35 and 1.25 M_{\odot} mass, respectively.

In a classical nova, such a short-lived UV-flash precedes the discovery of the nova at optical wavelengths by \sim one day, and will go unnoticed while traveling through the empty circumstellar space. On the contrary, in a symbiotic nova, the RG wind that permeates the circumstellar space absorbs the photons of the UV-flash and get ionized. The ionized gas starts immediately to recombine, glowing very brightly in the process. The recombination time scale (in hours) goes as $t_{\text{rec}} = 0.66 T_e^{0.8} n_e^{-1}$ (Ferland, 2003), where T_e is the electron temperature in 10^4 K units, and n_e is the electron density in 10^9 cm^{-3} units. Both lines and continuum are emitted by the recombining wind.

EMISSION LINES. The emission lines component from the flashed wind are quite sharp (FWHM $\sim 40 \text{ km sec}^{-1}$, as the outflow velocity of the RG wind is rather low), and are visible on-top the broad pedestal originating from the fast expanding ejecta (see top-left of Fig. 2). The evolution of the recombining H α component over the first few days of the V407 Cyg (2010), RS Oph (2021), and V3890 Sgr (2019) outbursts is compared in Fig. 2. The e-folding recombination times are respectively 100, 60 and 13 hours, corresponding to electronic densities of 6.6×10^6 , 1.1×10^7 and $5.0 \times 10^7 \text{ cm}^{-3}$. From Fig. 2 it is clear that prompt access to a telescope with a standing-by high-resolution spectrograph (resolving power $\geq 20,000$) is mandatory to successfully detect the presence of emission lines from the recombining wind and record the details of their very fast evolution.

The narrow emission lines from the flashed wind are invariably accompanied by a similarly sharp and slightly blue-shifted *absorption* component. It originates from the outer parts of the slowly outflowing RG wind, which remains neutral through the recombination process (which is equivalent to say that there is enough column density in the circumstellar material to absorb *all* the ionizing photons emitted during the initial UV-flash). While the narrow emission component traces gas which is roughly symmetric around the central binary, the blue-shifted narrow absorption provides a measure of the terminal wind velocity (at least in the direction probed by the line-of-sight to the observer). From the spectra in Fig. 2, such terminal wind velocity is -38 , -60 , and -65 km sec^{-1} for V407 Cyg, RS Oph, and V3890 Sgr, respectively.

NEBULAR CONTINUUM. If the passage of a classical nova at peak optical brightness corresponds to the maximum angular extension of the optically-

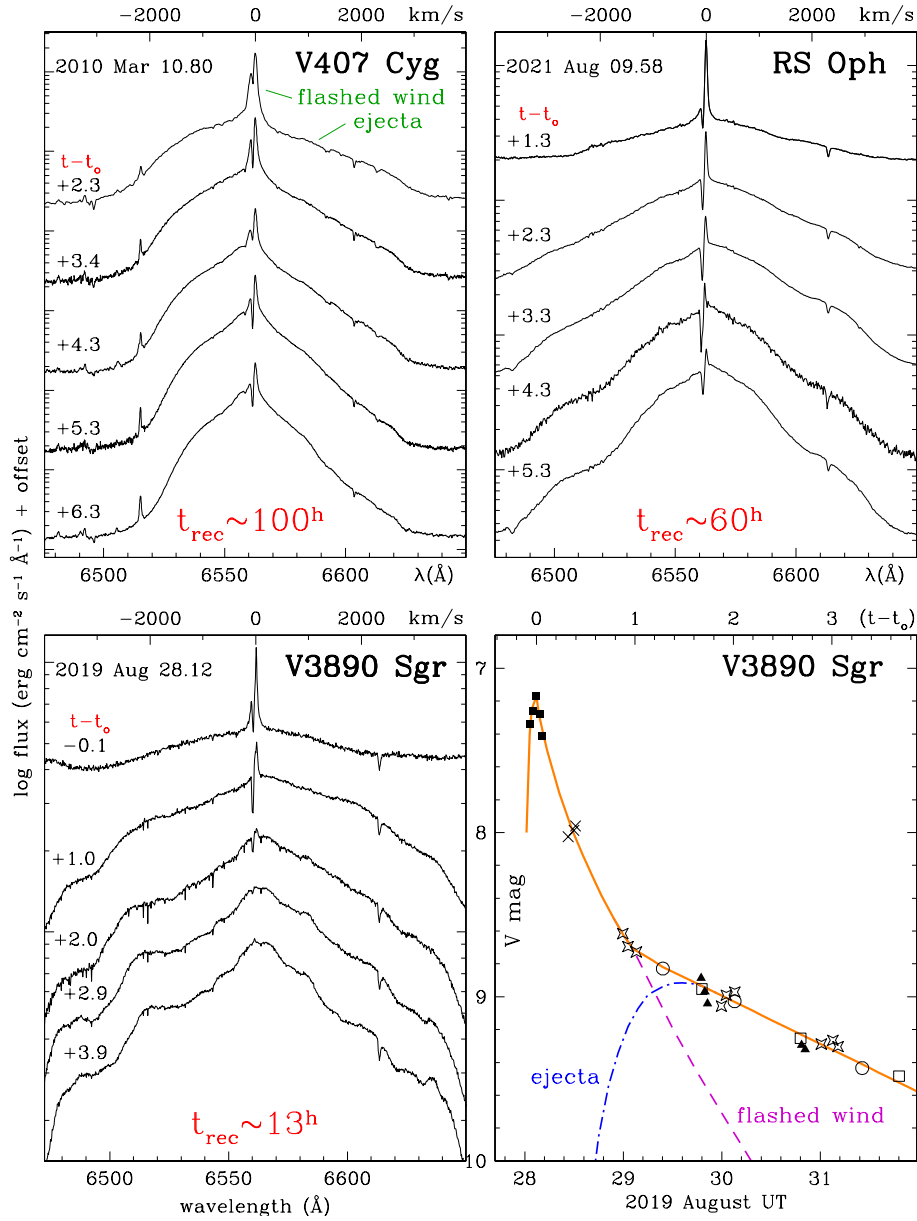


Figure 2. High-resolution H α profiles covering the first days for the outburst of three symbiotic novae, to highlight the sharp component from the recombining flashed-wind of the RG and the broad one from the expanding ejecta. For comparison, the early photometric evolution of V3890 Sgr is deconvolved into the same two components (data from [Munari et al., 2011](#); [Munari & Valisa, 2021](#), F. Walter private comm.)

thick pseudo-photosphere of the expanding ejecta, in a symbiotic nova it generally marks the time when the continuum radiation from the recombining wind reaches its peak output, roughly corresponding to the maximum mass reached by the ionized fraction of the RG wind. For ex., in the case of the 2019 outburst of V3890 Sgr, the continuum emission from flashed wind reached a peak brightness about $4\times$ that of the ejecta, as illustrated by the deconvolution of the V -band lightcurve in Fig. 2. The recombination time of the flashed wind is, unsurprisingly, the same if estimated from the continuum emission or from the narrow $H\alpha$ component, as illustrated for V3890 Sgr in Fig. 2, providing in both cases an e -folding time of ~ 13 hours.

RADIO THERMAL EMISSION. The UV-flashed wind of the RG emits free-free radiation that should be detectable at radio wavelengths within 1-2 days of TNR onset, before the stronger synchrotron emission from the shocked ejecta takes over. The geometrical arrangement and flux level for this prompt free-free radio emission should be similar to that of the RG wind kept ionized by the long-term burning WDs in SETE objects, which has been modeled by Taylor & Seaquist (1984), among others. A fair fraction of symbiotic stars with burning WDs is radio-emitter at cm-wavelengths, with brightness temperature and α spectral index ($S_\nu \propto \nu^\alpha$) suggestive of thermal emission from an outflowing wind (eg. Seaquist et al., 1984; Seaquist & Taylor, 1990; Seaquist et al., 1993). The main difficulty to observe at radio wavelengths this prompt free-free emission resides in the (very) fast response time required to access suitable radio telescopes before the recombination wave (proceeding inside-out because of the density gradient in the RG wind) completes its job and the synchrotron emission from the shocked ejecta takes over.

The earliest radio observation for the 2014 outburst of V745 Sco started 2.6 days past optical maximum (Molina et al., 2024), 2.0 days for V3890 Sgr in 2019 (Nyamai et al., 2023), and 2 to 5 days for RS Oph in 2021 (Williams et al., 2021; Sokolovsky et al., 2021). They all were already affected by the rapidly growing contribution of the synchrotron emission from the shocked ejecta, at an epoch when the thermal emission from the flashed wind was declining if not already extinguished. Better luck could favor the coming and much anticipated outburst of T CrB (in 2025-2026 ?), for which proposals have been approved at basically all radio facilities to be triggered by the announcement of a new outburst. A few of them specifically aim to obtain a "picture at rest" of the circumstellar medium before the ejecta will slam onto it, by imaging the prompt free-free thermal emission from the UV-flashed wind within hours of the outburst discovery.

3.2. Deceleration of the ejecta by the red giant wind

The second feature unique to symbiotic novae is the violent deceleration of the nova ejecta as they plow through the pre-existing circumstellar material, fed by the slow wind of the RG. The ejecta are shocked and give origin to copious non-thermal emission over the entire wavelength range, from radio synchrotron to the

TeV energies mapped by Cherenkov telescopes (Acciari et al., 2022; H. E. S. S. Collaboration et al., 2022). For RS Oph, the multi-wavelength results gathered from the 2006 and 2021 eruptions are very similar, which may be read as an indication that the cavity shaped by preceding eruptions is refilled by the wind of the red giant well in time for the following outburst, a results probably applicable also to the other symbiotic novae that were less intensively observed compared to RS Oph.

DEOP. The multi-wavelength appearance and fate of the shocked ejecta rest ultimately with the geometric arrangement of the circumstellar medium. Without the presence of the WD companion, the wind of the RG would fill the circumstellar space in a roughly spherically-symmetric manner. The gravitational pull of the WD deflects instead toward the orbital plane the mass-loss from the RG (eg. Mohamed & Podsiadlowski, 2012; Skopal & Cariková, 2015), creating a *Density Enhancement on the Orbital Plane* (DEOP). The more wind is deflected toward DEOP, the less is left to flow perpendicular to the orbital plane: ejecta launched into polar directions then suffer from only limited deceleration, while those on the orbital plane slam onto a much denser medium able to efficiently absorb (all) their kinetic momentum. For a given WD mass and RG mass-loss rate, a WD orbiting closer to the RG is more efficient in deflecting the RG wind away from polar directions and onto DEOP.

BIPOLAR RADIO-SYNCHROTRON LOBES. Direct imaging of the expanding ejecta of RS Oph, years past the 2006 outburst, have been obtained with HST in [OIII] 5007 line (Ribeiro et al., 2009) and with Chandra in X-rays (Montez et al., 2022). Detecting such faint signals from years-old ejecta requires careful PSF-subtraction and image deconvolution. More direct and detailed images of the expanding ejecta can be obtained in the radio with VLBI techniques (very long baseline interferometry). Their milli-arcsec capabilities allow prompt resolution of the structure of the ejecta already within a few weeks of the eruption. An example of the results obtained with EVN (European VLBI Network) for the outbursts of V407 Cyg (2010) and RS Oph (2021) are shown in Fig. 3: the radio-emitting ejecta are shaped into wide bipolar lobes expanding perpendicularly to DEOP. The radio emission is of synchrotron origin, as supported by the absorption-corrected α spectral slope and by the huge brightness temperature ($10^7/10^8$ K), which is orders of magnitude hotter than associated to thermal processes (10^4 K).

The angular expansion of radio lobes can be transformed into corresponding space velocity by knowledge of the distance and the orbital inclination, fairly well known for both V407 Cyg and RS Oph (4.0 and 2.7 kpc, $\sim 80^\circ$ and 57° ¹, respectively). The time dependence of the space velocity of their radio lobes is compared in Fig. 4. The radio lobes of RS Oph have kept expanding at a high and constant $v_{exp}=8150 \text{ km s}^{-1}$ space velocity since the earliest radio epoch

¹The orbital inclination of RS Oph is here revised from $i=54^\circ$ derived by Munari et al. (2022) to $i=57^\circ$ by considering the improved radio angular expansion rates from Lico et al. (2024).

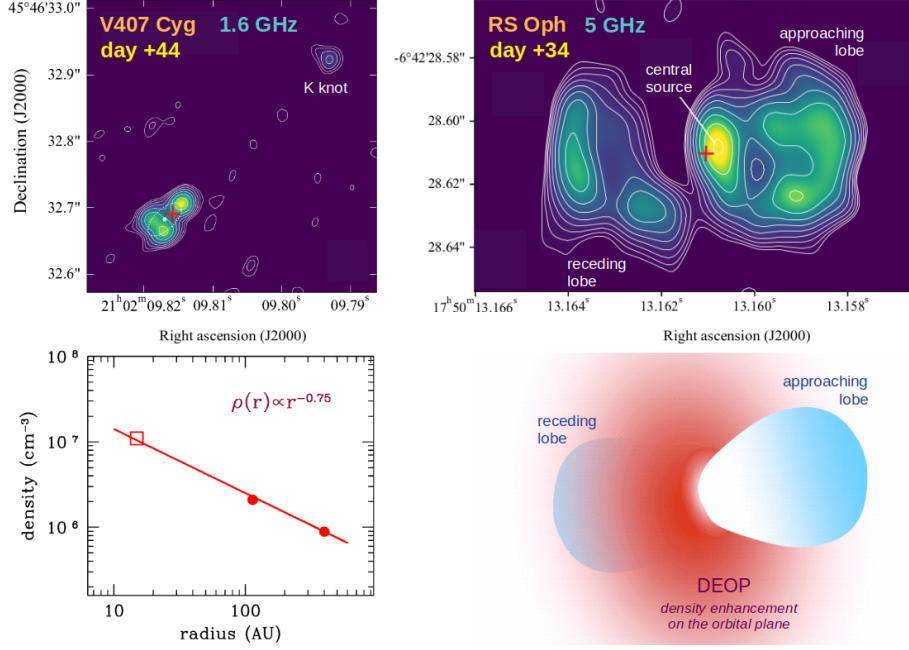


Figure 3. Top: VLBI high resolution radio maps of the 2010 and 2021 outbursts of the symbiotic novae V407 Cyg and RS Oph. The red cross marks the astrometric position from Gaia. Bottom right: cartoon highlighting the location of DEOP and the extinction it excerpts on the receding lobe of RS Oph (compare with panel directly above). Bottom left: the radial dependence of density within DEOP of RS Oph (data from Giroletti et al., 2020; Munari et al., 2022; Lico et al., 2024).

(day +14), which indicates that (i) the deceleration along the polar directions was completed already within the first two weeks, (ii) the WD orbiting close to the RG (1.5 AU orbital separation, Brandi et al., 2009) has been very effective in deflecting toward DEOP the wind of the RG, with a minimal amount of material present above 50 AU on the polar directions, and (iii) the terminal space velocity of the radio lobes is still a fairly large fraction of the initial launch velocity. The radio lobes of V407 Cyg have been instead decelerating all the way through the radio observing epochs, slowing from 6000 km s⁻¹ on day +20 to 2800 km s⁻¹ on day +91. This leads to conclude that the WD orbiting the RG at great distance (> 30 AU orbital separation, Hinkle et al., 2013) was not particularly effective in deflecting the wind of the RG away from polar directions, with enough gas still present 250 AU above DEOP to keep the ejecta of V407 Cyg decelerating for months. Considering the velocities observed in RS Oph and V407 Cyg, and the respective deceleration profiles, it seems safe to infer that the initial launch

velocity was similar for them both and probably close to $10,000/12,000 \text{ km s}^{-1}$.

The radio lobes of RS Oph, thanks to the 57° orbital inclination, have allowed to directly "see" DEOP for the first time in a symbiotic system. DEOP in RS Oph has been kept ionized by the WD burning nuclearly for the first three months of the outburst, so covering the whole set of radio observing epochs (day +14 to +64). An ionized DEOP is very effective in producing free-free absorption of the synchrotron radiation from the receding lobe which moves in the background to DEOP. Because the density within DEOP declines radially away from the central binary (cf. the lower-left panel of Fig. 3), also the free-free opacity declines in pace, with the net result that the receding lobe becomes visible only once its leading edge has moved behind DEOP outer regions of sufficiently low optical depth, which happens around day +20/+21, following the geometrical arrangement sketched in the lower-right panel of Fig. 3.

Before leaving this section about large-scale radio structures, it is worth mentioning an interesting and unexpected feature visible in the radio map of Fig. 3 for V407 Cyg: a knot of emission (labelled "K"), appears moving radially away - and along the same direction as the bipolar lobes - at a velocity (700 km sec^{-1}) that projects it back to the central binary ~ 6.5 yrs before the 2010 eruption, when V407 Cyg was undergoing a spectacular surge in the accretion rate onto the WD (Kolotilov et al., 2003), similar to what happened to T CrB in the 8 yrs preceding its 1946 outburst (Payne-Gaposchkin & Wright, 1946). Clearly, during such super-active accretion phases (SAP) preceding the nova explosion, the WD of symbiotic novae can expel isolated and massive blobs of material along the orbital polar axes. It will be worth searching for similar blobs on radio maps collected at the time of the next eruption of T CrB, considering the new SAP phase it has recently undergone during 2015-2023 (Munari et al., 2016). It will also be worth to re-inspect the abundant spectroscopic material collected during the SAP phase of V407 Cyg (eg. Tatarnikova et al., 2003) and search for spectral counterparts to the ejection of the "K" radio blob.

SHRINKING OF EMISSION LINES. An easily observable manifestation of the violent deceleration of the ejecta in a symbiotic nova is the rapid narrowing of the *broad component* (cf. identification at top-left of Fig. 2) of the emission lines (eg. Shore et al., 2011; Munari et al., 2011; Banerjee et al., 2014). The left panels of Fig. 4 show the shrinking of $H\alpha$ for the recent outbursts of V407 Cyg and RS Oph, characterized by slopes ($\text{FWHM} \propto t^\theta$) of $\theta = -0.59$ and -0.73 , respectively [for simplicity, in the rest of this paper $H\alpha$ will be used as proxy for permitted emission lines in general]. The narrowing of $H\alpha$ proceeds very smoothly, supporting an origin in ejecta that expand through a medium that extends also very smoothly over the traveled distance, without discontinuities or sudden changes in the radial density gradient. By integrating over the behavior in Fig. 4, and taking $v_{exp} = \text{FWHM}/2.355$ (i.e. the σ of the Gaussian fitting) as representative of the bulk velocity of the gas, the distance traveled by the $H\alpha$ emitting ejecta in the first 100 days is 15 and 14 AU for V407 Cyg and RS Oph, respectively. Such a limited dimension fits very nicely with the central

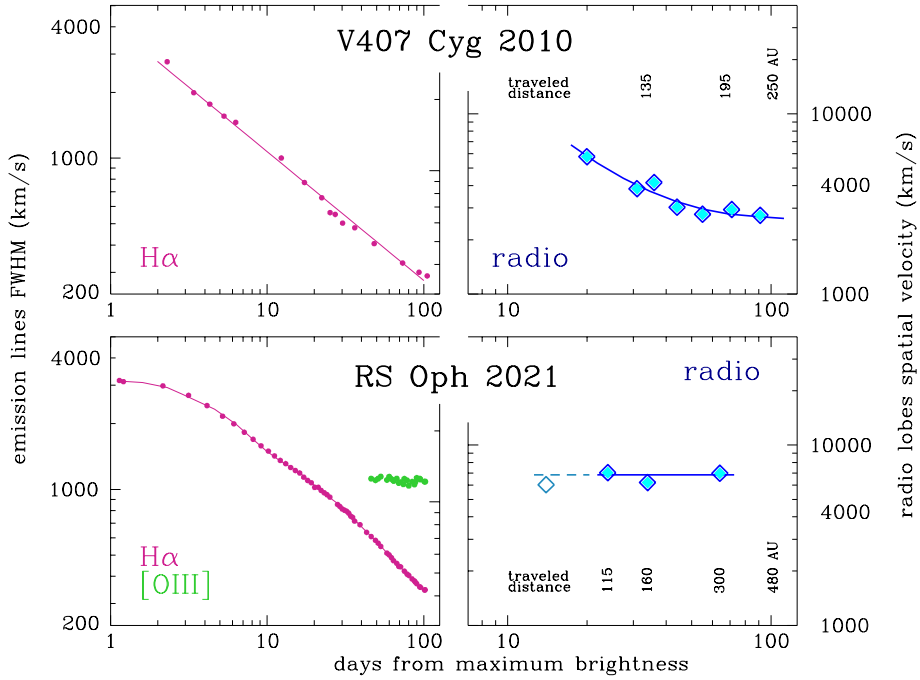


Figure 4. Comparing the evolution of the FWHM of Balmer and [OIII] emission lines (left) and the space velocity of the radio bipolar jets (right) for V407 Cyg and RS Oph (data from [Munari et al., 2011](#); [Giroletti et al., 2020](#); [Munari & Valisa, 2022](#); [Lico et al., 2024](#)).

synchrotron radio source (cf upper-right of Figure 3) of RS Oph, that when visible for the first 40 days past the initial outburst remained unresolved at the EVN restoring ellipsoidal beam of 10×12 milli-arcsec, corresponding to an upper limit of 13 AU to its radius. The fact that over the initial 100 days the radio lobes travel for 250-500 AU in the polar directions, while the H α emitting ejecta cover just 14-15 AU under constant deceleration, clearly indicates that the (main) source of H α emission is the ejecta moving close to the orbital plane and slamming onto DEOP.

3.3. X-rays

The evolution in X-rays of RS Oph has been monitored at \sim daily cadence with the *Swift* satellite for both the 2006 and 2021 outbursts. The energy distributions of X-rays have been deconvolved into hard and supersoft components by [Page et al. \(2022\)](#), from which we import the data plotted on the top row of Fig. 5.

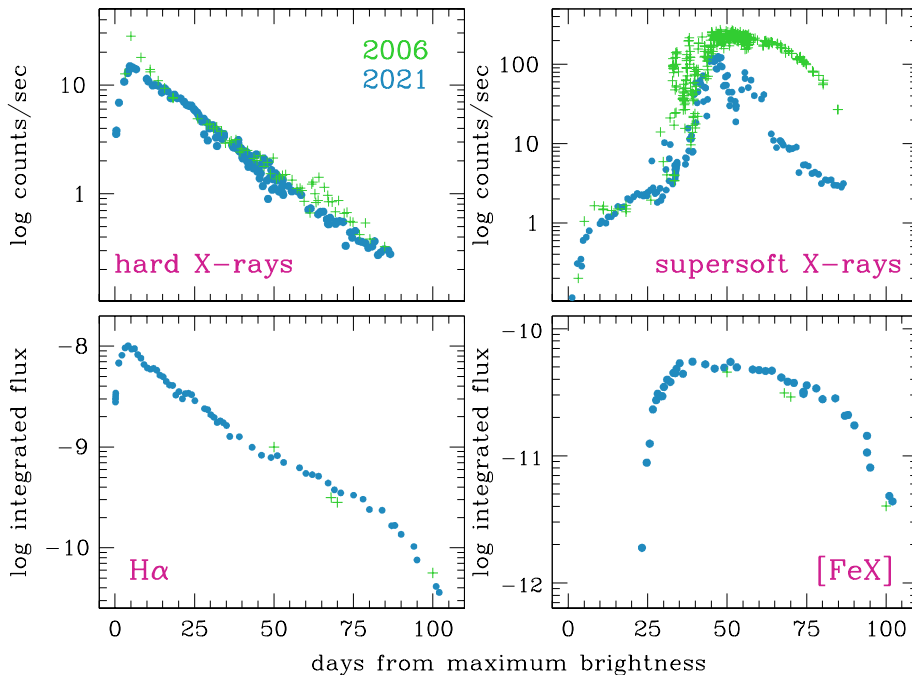


Figure 5. Comparing the evolution in flux for the 2006 and 2021 outbursts of RS Oph for hard X-rays, super-soft X-rays, permitted and coronal emission lines (data from Page et al., 2022; Munari & Valisa, 2022). The fluxes of optical emission lines are in $\text{erg cm}^{-2} \text{s}^{-1}$.

SUPERSOFT X-RAYS. They come directly from the central WD which is burning nuclearly at the surface, and become visible around day +25 when the medium around the WD clears enough to turn optically thin. Coronal emission lines appear at the same time (cf. the flux evolution of [FeX] 6375 Å plotted in the lower-right panel of Fig. 5), because they form in the circumstellar material now exposed to the hard radiation emanating from the burning WD. The coronal emission lines behaved very smoothly with time and very similar for the 2006 and 2021 eruptions, supporting identical burning phases on the WD for the two outbursts. The sharp decline in flux of the coronal lines suggests that the nuclear burning ends around day +85, which also coincides with the drop in supersoft X-rays observed during the 2006 event.

The excitation of coronal lines integrates the WD output over the 4π solid angle, and such lines are therefore well suited to trace the real output of the burning WD. On the contrary, supersoft X-rays - which are seen coming directly from the burning WD - are particularly sensitive to inhomogeneities in the absorbing material crossing the line-of-sight. This explains the rapid switch on/off

episodes at the start of the SSS phase in 2006 (Osborne et al., 2011). On the contrary, the SSS started smoothly in 2021 but significantly under-performed at later epochs compared to 2006; such difference has been modeled by Ness et al. (2023) in terms of different column density of absorbing material at the two outbursts. The opposite behavior of supersoft X-rays seen in 2006 and 2021, both during their rise to maximum and decline from, probably relates to the fact that the WD+RG binary was at opposite orbital phases at the time of the two eruptions. Therefore the line-of-sight to the WD may have probed at grazing incidence, in one eruption the inner wall of the cavity shaped into DEOP by the ejecta, and instead the outer atmosphere/inner wind of the RG at the other.

HARD X-RAYS. The hard X-rays originate from the ejecta colliding with the pre-existing material. The flux evolution of hard X-rays is identical for 2006 and 2021 (upper-left panel of Fig. 5), suggesting that RG wind had similarly refilled the circumstellar space after the previous eruption and that the ejecta impacted with the same mass and velocity (momentum). The decline in hard X-ray is continuous, very smooth, and without glitches, indicating a similarly smooth, continuous and extended distribution of the target slow material. This is the same conclusion we drawn above from the FWHM evolution of $H\alpha$, a fact suggesting that $H\alpha$ and hard X-rays come from the same location within the binary system. This is also supported by the time-dependence of the *flux* radiated in $H\alpha$, which is plotted in the lower-left panel of Fig. 5, which is exactly the same as that of hard X-rays from the panel above.

3.4. Summary: a multi-wavelength 3D picture

Putting all together the information from the previous sections about the size, velocity and time evolution at radio, optical, and X-rays, a 3D picture of RS Oph (serving also as a guideline for symbiotic novae in general) can be assembled as illustrated in Fig. 6.

The WD ejecta are launched symmetrically by the WD at 10,000 to 12,000 km sec^{-1} initial velocity. They interact with the pre-existing circumstellar material primarily at two distinct locations.

One location is very close to the central binary, at the inner radius of DEOP (the density enhancement on the orbital plane formed by the gravitational focusing of the RG wind by the orbiting WD). The high density and long radial extent of DEOP keeps the ejecta decelerating very smoothly for weeks/months, and the shock interface travels only a short distance, ~ 15 AU in 100 days at which point the ejecta have been practically arrested (velocities $\leq 150 \text{ km sec}^{-1}$). The DEOP/ejecta interface is the location from where originates most of the hard X-rays, the central radio-synchrotron component, and the permitted optical emission lines. This interface is also probably the place where the high-energy γ -rays (visible in the first days of the outburst) are produced.

The other location is toward the poles of the orbital plane, where the density of pre-existing material is much lower compared to DEOP. Perpendicular to the

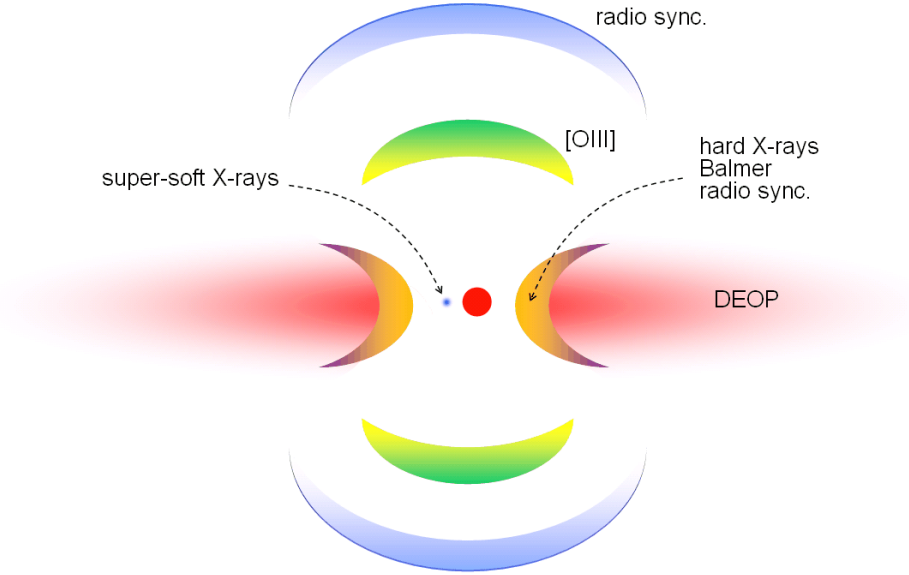


Figure 6. Artistic impression showing the location of key emission features in RS Oph around day +35 of the outburst (drawing not to scale). The WD + RG binary is at the center, DEOP (density enhancement on the orbital plane) is seen edge-on, and the polar directions run vertically.

orbital plane the deceleration is much less effective, and the ejecta launched in that direction, after 100 days are still traveling at thousands of km sec^{-1} , having crossed hundreds of AU. The shocked outer edge of the resulting bipolar lobes is the location of the synchrotron emission dominating at radio cm-wavelengths.

The forbidden emission lines are observed in RS Oph to move at constant and high velocity, much larger than for permitted lines, as illustrated in the lower-left panel of Fig. 4. With all probability they form in the inner regions of the bipolar lobes, which move at a reduced velocity compared with their outer edges, turning visible once the local density dilutes below the critical value for collisional de-excitation of their upper metastable levels.

The cavity in the pre-existing circumstellar material shaped by ejecta plowing through them is efficiently and quickly refilled by the wind of the red giant: each outburst of RS Oph has behaved exactly the same, even those separated by just 9 years (like 1958 and 1967). The accretion disk around the WD is even quicker to reform, ~ 250 days being enough to restore both pre-outburst disk brightness and flickering activity (Munari & Tabacco, 2022).

4. An imminent eruption of T CrB ?

The two known outbursts of T CrB in 1866 and 1946 are separated by 80 yrs, and other 80yrs will bring us to 2026. The 1946 eruption was preceded by a SAP phase lasting ~ 8 yrs, and a new SAP characterized T CrB from 2015 to 2023 (Munari et al., 2016) leading to the natural conclusion that a new eruption may be imminent. Such a view has been shared by many (eg. Schaefer, 2023; Zamanov et al., 2023), with the beneficial results of an intensified pre-eruption monitoring of T CrB and the submission of proposals to most of the ground and space observing facilities; proposals waiting to be triggered at the very first announcement of the outburst ! Such an alertness from the community, the expected peak $V \sim 3$ mag brightness, and the proximity of T CrB to us (just 0.9 kpc distance and negligible interstellar reddening), with all probabilities will result in such a wealth of multi-wavelength information to keep people busy for long in understanding and modeling them, leading to a significant leap forward in our understanding of novae in general and their symbiotic subclass in particular.

Acknowledgements. We acknowledge the INAF 2023 Minigrant funding program and the Conference Organizers for financial support. We thank K. Page, F. Walter, R. Lico, and P. Valisa for permission to use their data in drawing some of the figures.

References

- Abdo, A. A., Ackermann, M., Ajello, M., et al., Gamma-Ray Emission Concurrent with the Nova in the Symbiotic Binary V407 Cygni. 2010, *Science*, **329**, 817, DOI: 10.1126/science.1192537
- Acciari, V. A., Ansoldi, S., Antonelli, L. A., et al., Proton acceleration in thermonuclear nova explosions revealed by gamma rays. 2022, *Nature Astronomy*, **6**, 689, DOI: 10.1038/s41550-022-01640-z
- Allen, D. A., On the late-type components of slow novae and symbiotic stars. 1980, *Monthly Notices of the RAS*, **192**, 521, DOI: 10.1093/mnras/192.3.521
- Arseneau, S., Chandra, V., Hwang, H.-C., et al., Measuring the Mass–Radius Relation of White Dwarfs Using Wide Binaries. 2024, *Astrophysical Journal*, **963**, 17, DOI: 10.3847/1538-4357/ad2168
- Banerjee, D. P. K., Joshi, V., Venkataraman, V., et al., Near-IR Studies of Recurrent Nova V745 Scorpii during its 2014 Outburst. 2014, *Astrophysical Journal, Letters*, **785**, L11, DOI: 10.1088/2041-8205/785/1/L11
- Bode, M. F. & Evans, A., eds. 1989, *Classical novae* (John Wiley & Sons)
- Bode, M. F. & Evans, A., eds. 2008, *Classical Novae* (Cambridge Univ. Press)
- Brandi, E., Quiroga, C., Mikołajewska, J., Ferrer, O. E., & García, L. G., Spectroscopic orbits and variations of RS Ophiuchi. 2009, *Astronomy and Astrophysics*, **497**, 815, DOI: 10.1051/0004-6361/200811417

- Cassatella, A., González-Riestra, R., & Selvelli, P., eds. 2004, ESA Special Publication, Vol. **1283**, *INES Access Guide No. 3 - Classical Novae*
- Cassatella, A., Selvelli, P. L., Gilmozzi, R., Bianchini, A., & Friedjung, M., IUE observations of faint old novae. 1990, in *Accretion-Powered Compact Binaries*, ed. C. W. Mauche (Cambridge Univ. Press), 373–376
- Cassatella, A. & Viotti, R., eds. 1990, Lecture Notes in Physics, Vol. **369**, *Physics of Classical Novae* (Springer-Verlag)
- Downes, R., Webbink, R. F., & Shara, M. M., A Catalog and Atlas of Cataclysmic Variables-Second Edition. 1997, *Publications of the ASP*, **109**, 345, DOI: 10.1086/133900
- Downes, R. A. & Shara, M. M., A Catalog of Cataclysmic Variables. 1993, *Publications of the ASP*, **105**, 127, DOI: 10.1086/133139
- Downes, R. A., Webbink, R. F., Shara, M. M., et al., A Catalog and Atlas of Cataclysmic Variables: The Living Edition. 2001, *Publications of the ASP*, **113**, 764, DOI: 10.1086/320802
- Duerbeck, H. W. 1987, *A reference catalogue and atlas of galactic novae* (D. Reidel Publ.)
- Evans, A., Bode, M. F., O'Brien, T. J., & Darnley, M. J., eds. 2008, Astronomical Society of the Pacific Conference Series, Vol. **401**, *RS Ophiuchi (2006) and the Recurrent Nova Phenomenon*
- Ferland, G. J., Quantitative Spectroscopy of Photoionized Clouds. 2003, *Annual Review of Astron and Astrophys*, **41**, 517, DOI: 10.1146/annurev.astro.41.011802.094836
- Fujimoto, M. Y., A Theory of Hydrogen Shell Flashes on Accreting White Dwarfs - Part Two - the Stable Shell Burning and the Recurrence Period of Shell Flashes. 1982a, *Astrophysical Journal*, **257**, 767, DOI: 10.1086/160030
- Fujimoto, M. Y., A theory of hydrogen shell flashes on accreting white dwarfs. I - Their progress and the expansion of the envelope. II - The stable shell burning and the recurrence period of shell flashes. 1982b, *Astrophysical Journal*, **257**, 752, DOI: 10.1086/160029
- Gaia Collaboration, The Gaia mission. 2016, *Astronomy and Astrophysics*, **595**, A1, DOI: 10.1051/0004-6361/201629272
- Gaia Collaboration, Gaia Data Release 3. Summary of the content and survey properties. 2023, *Astronomy and Astrophysics*, **674**, A1, DOI: 10.1051/0004-6361/202243940
- Gaposchkin, C. H. P. 1957, *The Galactic Novae* (Dover Pub.)
- Giroletti, M., Munari, U., Körding, E., et al., Very long baseline interferometry imaging of the advancing ejecta in the first gamma-ray nova V407 Cygni. 2020, *Astronomy and Astrophysics*, **638**, A130, DOI: 10.1051/0004-6361/202038142
- H. E. S. S. Collaboration, Aharonian, F., Ait Benkhali, F., et al., Time-resolved hadronic particle acceleration in the recurrent nova RS Ophiuchi. 2022, *Science*, **376**, 77, DOI: 10.1126/science.abn0567

- Hernanz, M. & José, J., eds. 2002, American Institute of Physics Conference Series, Vol. **637**, *Classical Nova Explosions* (AIP)
- Hinkle, K. H., Fekel, F. C., Joyce, R. R., & Wood, P., Infrared Spectroscopy of Symbiotic Stars. IX. D-type Symbiotic Novae. 2013, *Astrophysical Journal*, **770**, 28, DOI: 10.1088/0004-637X/770/1/28
- Iben, I., J., Hot accreting white dwarfs in the quasi-static approximation. 1982, *Astrophysical Journal*, **259**, 244, DOI: 10.1086/160164
- Kenyon, S. J. 1986, *The symbiotic stars* (Cambridge Univ. Press)
- Kenyon, S. J. & Truran, J. W., The outbursts of symbiotic novae. 1983, *Astrophysical Journal*, **273**, 280, DOI: 10.1086/161367
- Kolotilov, E. A., Shenavrin, V. I., Shugarov, S. Y., & Yudin, B. F., UBVJHKLM photometry of the symbiotic Mira V407 Cyg in 1998 2002. 2003, *Astronomy Reports*, **47**, 777, DOI: 10.1134/1.1611218
- Lico, R., Giroletti, M., Munari, U., et al., High-resolution imaging of the evolving bipolar outflows in symbiotic novae: The case of the RS Ophiuchi 2021 nova outburst. 2024, *Astronomy and Astrophysics*, **692**, A107, DOI: 10.1051/0004-6361/202451364
- Liimets, T., Corradi, R. L. M., Santander-García, M., et al., A Three-dimensional View of the Remnant of Nova Persei 1901 (GK Per). 2012, *Astrophysical Journal*, **761**, 34, DOI: 10.1088/0004-637X/761/1/34
- Mohamed, S. & Podsiadlowski, P., Mass Transfer in Mira-type Binaries. 2012, *Baltic Astronomy*, **21**, 88, DOI: 10.1515/astro-2017-0362
- Molina, I., Chomiuk, L., Linford, J. D., et al., The symbiotic recurrent nova V745 Sco at radio wavelengths. 2024, *Monthly Notices of the RAS*, **534**, 1227, DOI: 10.1093/mnras/stae2093
- Montez, R., Luna, G. J. M., Mukai, K., Sokoloski, J. L., & Kastner, J. H., Expanding Bipolar X-Ray Structure After the 2006 Eruption of RS Oph. 2022, *Astrophysical Journal*, **926**, 100, DOI: 10.3847/1538-4357/ac4583
- Munari, U., The Symbiotic Stars. 2019, in *The Impact of Binary Stars on Stellar Evolution*, ed. G. Beccari & H. Boffin, arXiv:1909.01389
- Munari, U., Dallaporta, S., & Cherini, G., The 2015 super-active state of recurrent nova T CrB and the long term evolution after the 1946 outburst. 2016, *New Astronomy*, **47**, 7, DOI: 10.1016/j.newast.2016.01.002
- Munari, U., Giroletti, M., Marcote, B., et al., Radio interferometric imaging of RS Oph bipolar ejecta for the 2021 nova outburst. 2022, *Astronomy and Astrophysics*, **666**, L6, DOI: 10.1051/0004-6361/202244821
- Munari, U., Joshi, V. H., Ashok, N. M., et al., The 2010 nova outburst of the symbiotic Mira V407 Cyg. 2011, *Monthly Notices of the RAS*, **410**, L52, DOI: 10.1111/j.1745-3933.2010.00979.x
- Munari, U. & Tabacco, F., Flickering Returns as RS Oph Reestablishes Quiescent Conditions Following its 2021 Nova Outburst. 2022, *Research Notes of the American Astronomical Society*, **6**, 103, DOI: 10.3847/2515-5172/ac72ae

- Munari, U., Traven, G., Masetti, N., et al., The GALAH survey and symbiotic stars - I. Discovery and follow-up of 33 candidate accreting-only systems. 2021, *Monthly Notices of the RAS*, **505**, 6121, DOI: 10.1093/mnras/stab1620
- Munari, U. & Valisa, P., The 2021 outburst of RS Oph. A pictorial atlas of the spectroscopic evolution: the first 18 days. 2021, *arXiv e-prints*, arXiv:2109.01101, DOI: 10.48550/arXiv.2109.01101
- Munari, U. & Valisa, P., The 2021 outburst of RS Oph: a pictorial atlas of the spectroscopic evolution. II. From day 19 to 102 (solar conjunction). 2022, *arXiv e-prints*, arXiv:2203.01378, DOI: 10.48550/arXiv.2203.01378
- Ness, J. U., Beardmore, A. P., Bode, M. F., et al., High-resolution X-ray spectra of RS Ophiuchi (2006 and 2021): Revealing the cause of SSS variability. 2023, *Astronomy and Astrophysics*, **670**, A131, DOI: 10.1051/0004-6361/202245269
- Nyamai, M. M., Linford, J. D., Allison, J. R., et al., Synchrotron emission from double-peaked radio light curves of the symbiotic recurrent nova V3890 Sgr. 2023, *Monthly Notices of the RAS*, **523**, 1661, DOI: 10.1093/mnras/stad1534
- O'Brien, T. & Bode, M., Resolved nebular remnants. 2008, in *Classical Novae*, ed. M. F. Bode & A. Evans (Cambridge Univ. Press), 285–305
- Osborne, J. P., Page, K. L., Beardmore, A. P., et al., The Supersoft X-ray Phase of Nova RS Ophiuchi 2006. 2011, *Astrophysical Journal*, **727**, 124, DOI: 10.1088/0004-637X/727/2/124
- Page, K. L., Beardmore, A. P., Osborne, J. P., et al., The 2021 outburst of the recurrent nova RS Ophiuchi observed in X-rays by the Neil Gehrels Swift Observatory: a comparative study. 2022, *Monthly Notices of the RAS*, **514**, 1557, DOI: 10.1093/mnras/stac1295
- Payne-Gaposchkin, C. & Wright, F. W., The Photographic Light-Curve of T Coronae Borealis. 1946, *Astrophysical Journal*, **104**, 75, DOI: 10.1086/144834
- Ribeiro, V. A. R. M., Bode, M. F., Darnley, M. J., et al., The Expanding Nebular Remnant of the Recurrent Nova RS Ophiuchi (2006). II. Modeling of Combined Hubble Space Telescope Imaging and Ground-based Spectroscopy. 2009, *Astrophysical Journal*, **703**, 1955, DOI: 10.1088/0004-637X/703/2/1955
- Saikia, D. F. & Anupama, G. C., eds. 2012, *Bull. Astr. Soc. India*, Vol. **40**, *Novae from radio to gamma rays* (Astron. Soc. India)
- Schaefer, B. E., The B & V light curves for recurrent nova T CrB from 1842-2022, the unique pre- and post-eruption high-states, the complex period changes, and the upcoming eruption in 2025.5 ± 1.3 . 2023, *Monthly Notices of the RAS*, **524**, 3146, DOI: 10.1093/mnras/stad735
- Schwarz, G. J., Ness, J.-U., Osborne, J. P., et al., Swift X-Ray Observations of Classical Novae. II. The Super Soft Source Sample. 2011, *Astrophysical Journal, Supplement*, **197**, 31, DOI: 10.1088/0067-0049/197/2/31
- Seaquist, E. R., Krogulec, M., & Taylor, A. R., A Highly Sensitive Radio Survey of Symbiotic Stars at 3.6 Centimeters. 1993, *Astrophysical Journal*, **410**, 260, DOI: 10.1086/172742

- Seaquist, E. R. & Taylor, A. R., The Collective Radio Properties of Symbiotic Stars. 1990, *Astrophysical Journal*, **349**, 313, DOI: 10.1086/168315
- Seaquist, E. R., Taylor, A. R., & Button, S., A Radio Survey of Symbiotic Stars. 1984, *Astrophysical Journal*, **284**, 202, DOI: 10.1086/162399
- Shore, S. N., Wahlgren, G. M., Augusteijn, T., et al., The spectroscopic evolution of the symbiotic-like recurrent nova V407 Cygni during its 2010 outburst. I. The shock and its evolution. 2011, *Astronomy and Astrophysics*, **527**, A98, DOI: 10.1051/0004-6361/201015901
- Skopal, A. & Cariková, Z., Wind mass transfer in S-type symbiotic binaries. I. Focusing by the wind compression model. 2015, *Astronomy and Astrophysics*, **573**, A8, DOI: 10.1051/0004-6361/201424779
- Skopal, A., Shugarov, S. Y., Munari, U., et al., The path to Z And-type outbursts: The case of V426 Sagittae (HBHA 1704-05). 2020, *Astronomy and Astrophysics*, **636**, A77, DOI: 10.1051/0004-6361/201937199
- Skrutskie, M. F., Cutri, R. M., Stiening, R., et al., The Two Micron All Sky Survey (2MASS). 2006, *Astronomical Journal*, **131**, 1163, DOI: 10.1086/498708
- Sokoloski, J. L., Rupen, M. P., & Mioduszewski, A. J., Uncovering the Nature of Nova Jets: A Radio Image of Highly Collimated Outflows from RS Ophiuchi. 2008, *Astrophysical Journal, Letters*, **685**, L137, DOI: 10.1086/592602
- Sokolovsky, K., Aydi, E., Chomiuk, L., et al., VLA observations of the 2021 eruption of RS Oph. 2021, *The Astronomer's Telegram*, **14886**, 1
- Starrfield, S., Thermonuclear processes and the classical nova outburst. 1989, in *Classical Novae*, ed. M. F. Bode & A. Evans (John Wiley & Sons), 39–60
- Starrfield, S., Iliadis, C., & Hix, W. R., Thermonuclear processes. 2008, in *Classical Novae*, ed. M. F. Bode & A. Evans (Cambridge Univ. Press), 77–101
- Tatarnikova, A. A., Marrese, P. M., Munari, U., Tomov, T., & Yudin, B. F., Spectral observations of the symbiotic Mira variable V407 Cyg in 1993 2002. 2003, *Astronomy Reports*, **47**, 889, DOI: 10.1134/1.1626192
- Taylor, A. R. & Seaquist, E. R., Radio emission from symbiotic stars : a binary model. 1984, *Astrophysical Journal*, **286**, 263, DOI: 10.1086/162594
- Tomov, T. V., Stoyanov, K. A., & Zamanov, R. K., AG Pegasi - now a classical symbiotic star in outburst? 2016, *Monthly Notices of the RAS*, **462**, 4435, DOI: 10.1093/mnras/stw2012
- Warner, B. *Cataclysmic variable stars*, , Vol. **28** (Cambridge Univ. Press)
- Williams, D., O'Brien, T., Woudt, P., et al., AMI-LA, e-MERLIN and MeerKAT radio detections of RS Oph in outburst. 2021, *The Astronomer's Telegram*, **14849**, 1
- Woudt, P. A. & Ribeiro, V. A. R. M., eds. 2014, Astronomical Society of the Pacific Conference Series, Vol. **490**, *Stella Novae: Past and Future Decades*
- Zamanov, R., Boeva, S., Latev, G. Y., et al., Accretion in the recurrent nova T CrB: Linking the superactive state to the predicted outburst. 2023, *Astronomy and Astrophysics*, **680**, L18, DOI: 10.1051/0004-6361/202348372